Translational Diffusion of Linear Polystyrenes in Dilute and Semidilute Solutions of Poly(vinyl methyl ether)

L. M. Wheeler,† T. P. Lodge,*† B. Hanley,‡§ and M. Tirrell‡

Department of Chemistry and Department of Chemical Engineering and Materials Science, University of Minnesota, Minneapolis, Minnesota 55455. *Received August 22, 1986*

ABSTRACT: Translational diffusion coefficients are reported for trace amounts of linear polystyrenes (PS) in dilute and semidilute solutions of poly(vinyl methyl ether) (PVME), measured by dynamic light scattering. The PS molecular weights were 6.5×10^4, 1.79×10^5, 4.22×10^5, and 1.05×10^6, the PVME molecular weight was 1.3×10^6, and the PVME concentration ranged from 0.001 to 0.1 g/mL. The PS diffusion follows a molecular weight power law at all concentrations, with the exponent varying smoothly from −0.55 at infinite dilution to −1.9 at the highest concentration. Concentration scaling is obtained with overlap concentrations c^* calculated by assuming Θ solution conditions for the PS, implying a contraction of PS coil dimensions with increasing PVME concentration, even in the dilute regime. Estimates of the concentration for the onset of entanglement, c_e, indicate that $c > c_e$ is a minimum requirement for the observation of reptation. As $c_e > c^*$ in general, reptation may not be important in typical semidilute solutions. It is shown that a combination of reptation and constraint release cannot describe semidilute diffusion data, in contrast to the melt case; additional factors render the solution case more complicated to model. An empirical, stretched exponential scaling function does describe the concentration dependence of diffusion quite well, but the physical significance of this success may not be profound.

Introduction

Over the past decade, there has been considerable interest in the dynamics of concentrated polymer solutions and melts, largely inspired by de Gennes' postulate of reptation as the fundamental mechanism for polymer diffusion and relaxation in entangled systems.[1] In order to test the reptation model, there have been a number of studies of polymer translational diffusion, as a function of molecular weight, concentration, and topology. However, in spite of the growing amount of data, a complete understanding of the mechanisms of polymer motion has not yet been achieved.

Polymer solution behavior can be conveniently divided into three regimes: dilute, concentrated or melt, and the intermediate semidilute region. In dilute solution, the viscosity can be expressed as a series expansion in the polymer concentration, and translational diffusion coefficients follow the Stokes–Einstein relation. In entangled melts, diffusion of linear polymers is largely consistent with the M^{-2} power law, which may be considered the signature of reptation. However, the experimentally observed $M^{3.4}$ power law for shear viscosity in this regime is not consistent with the M^3 prediction of reptation. Consequently, there have been both modifications to the basic reptation hypothesis and also alternative relaxation mechanisms proposed, and the issue is not as yet resolved.

As a transition between the two limiting cases, it is reasonable to inquire whether an onset of reptation is observed in the semidilute region. Above the coil overlap concentration, c^*, polymer dynamics have been described in terms of reptation coupled with scaling theory.[2] The resulting predictions for the translational diffusion coefficient, D, are $D \sim M^{-2}c^{-1.75}$ for linear polymers in good solvents and $D \sim M^{-2}c^{-3}$ in Θ solvents. However, dynamics in semidilute solutions are even more complicated to model than in the melt since additional factors must be considered. For example, it may be necessary to account for the concentration dependence of the monomeric friction factor, the enhanced mobility of the molecules surrounding the test polymer, the relatively few entanglements per chain, and the changing effective solvent quality with increasing polymer concentration.

Experimental data in the semidilute region have yielded some apparently conflicting results and rather varying degrees of agreement with scaling theory. The subject has recently been reviewed,[3] and the following examples illustrate the range of results reported to date. Leger et al.[4] measured D for polystyrene in benzene solutions by forced Rayleigh scattering and found $D \sim M^{-2}c^{-1.75}$ as predicted by the scaling theory. Callaghan and Pinder,[5] however, reported that while log D vs. log c curves exhibit a slope of ≈ -1.75 at concentrations above $c/c^* \approx 5$, D scales as $M^{-1.4}$; the chemical system was polystyrene in carbon tetrachloride, and D was measured by pulsed-field gradient NMR. In 1984, Yu et al. reported diffusion data with a consistent M^{-2} dependence for polystyrene in tetrahydrofuran, also using forced Rayleigh scattering.[6] However, the concentration dependence did not fit a unique power law, and the slope of log D vs. log c became increasingly negative at high concentrations, reaching values of −13. More recently, Yu et al.[7] investigated the effect of matrix molecular weight, P, and found that the translational diffusion coefficient of the probe chain does not reach its large P limit, D_∞, until P is 3–5 times higher than the diffusant molecular weight, M. This violates the conditions for reptation, where D is independent of matrix molecular weight, and thus self-diffusion data ($P = M$) in semidilute solution may need reevaluation. Yu et al. also found no unique power law relationship for D_∞ as a function of M or c and hence question the role of reptation in the semidilute region.

Due to the complex nature of the semidilute regime, several other mechanisms may contribute to polymer diffusion and should be considered. For example, constraint release is a mode of relaxation that describes the lateral freedom of a test chain due to the reptation of neighboring chains. There is good evidence in melt data for both linear and branched polymers that constraint release can be quite significant.[8,9] Alternatively, the coupled motion of polymer chains has recently been modeled in terms of the "noodle effect", in which parts of the constraining chains are dragged along with a primary chain; this leads to a diffusion coefficient that varies as $D \sim M^{-2.5}c^{-1.5}$.[10] As in the dilute limit, polymers may also exhibit Stokes–Einstein type diffusion, governed by the

† Department of Chemistry.
‡ Department of Chemical Engineering and Materials Science.
§ Current address: Rohm & Haas Co., Bristol, PA 19007.

0024-9297/87/2220-1120$01.50/0

macroscopic solution viscosity and the hydrodynamic radius of the test chain. The effectiveness of the Stokes–Einstein mode presumably decreases drastically when the individual chains are fully interpenetrating, but it is not immediately clear at which concentration this occurs. One additional diffusion process to be considered is the random Brownian motion of a particle through a field of obstacles which generate hydrodynamic screening; this approach appears to be quite successful for describing the diffusion of globular or spherical objects in polymer solutions.[11-17] Along these lines, an alternative interpretation of diffusion in semidilute and dilute solutions has been suggested by Phillies.[18] The behavior of polymers and globular proteins (which cannot reptate) was compared, and literature values for D were fit to the empirical equation $D = D_0 \exp(-ac^u)$, where a and u are free parameters. On the basis of the ability of this function to describe the data for both types of solutions, it was concluded that polymers and proteins diffuse by the same mechanism and that reptation is not significant in semidilute solutions.

In an attempt to shed further light on the mechanisms of transport in semidilute solutions, this paper presents diffusion coefficients obtained by dynamic light scattering from ternary solutions. With this technique, the center-of-mass translation of a probe molecule can be measured in polymer solutions both above and below the overlap concentration.[19-24] In this instance, the probe is a trace quantity of polystyrene (PS) in isorefractive poly(vinyl methyl ether) (PVME)/*o*-fluorotoluene (*o*-FT) solutions. As PS/PVME form a compatible pair,[25,26] they are assumed to mix on a molecular level, and thus the behavior of the PS is taken to mimic diffusion in a binary solution. Four polystyrene samples were used, with molecular weights ranging from 6.5×10^4 to 1.05×10^6, and the matrix concentration range was 0.001–0.10 g/mL. The matrix molecular weight was 1.3×10^6, and thus the solutions are significantly entangled at the higher concentrations.

Experimental Section

Samples and Solutions. Details of the solution preparation protocol have been described previously.[27] Ternary solutions were prepared directly in scattering cells by mixing dilute, filtered solutions of PS/*o*-FT and PVME/*o*-FT. The solvent was then evaporated off slowly under flowing nitrogen until the desired PVME concentration was reached. The four linear polystyrene samples used were NBS 1479, $M_w = 1.05 \times 10^6$; Toyo-Soda F-40, $M_w = 4.22 \times 10^5$; NBS 705, $M_w = 1.79 \times 10^5$; Polysciences, $M_w = 6.5 \times 10^4$. All PS samples have a polydispersity of $M_w/M_n < 1.1$. The PVME, $M_w = 1.3 \times 10^6$, $M_w/M_n \approx 1.6$, is one of several high molecular weight fractions recently synthesized at NBS.[28] Diffusion coefficients were measured as a function of PVME concentration, ranging from the dilute (0.001 g/mL) to thoroughly entangled but still semidilute (0.1 g/mL). Solutions were diluted from the highest PVME concentration with filtered PS stock solutions to maintain a constant PS concentration. The mean and range of the PS concentrations for each set of samples were as follows: $M_w = 1.05 \times 10^6$, $c_{PS} = 0.460 \pm 0.02$ mg/mL; $M_w = 4.22 \times 10^5$, $c_{PS} = 0.764 \pm 0.08$ mg/mL; $M_w = 1.79 \times 10^5$, $c_{PS} = 0.975 \pm 0.1$ mg/mL; $M_w = 6.5 \times 10^4$, $c_{PS} = 3.07 \pm 0.1$ mg/mL. After dilution, each cell was mixed thoroughly and allowed to equilibrate. Equilibration times ranged from 3 days to several weeks, and measurements were repeated at 1-week intervals to check reproducibility and homogeneity. All measurements were made at 30.0 ± 0.1 °C, where $\partial n/\partial c$ for PVME/*o*-FT is less than 0.001; the corresponding quantity for PS/*o*-FT is approximately 0.1.

DLS Measurements. Correlation functions were obtained with a home-built spectrometer, and a 128-channel, multisample time correlator (Brookhaven Instruments BI-2030). Details of the apparatus appear elsewhere.[27] Correlation functions were collected in the homodyne mode at five or more angles, and the diffusion coefficient was obtained from the slope of $\bar{\Gamma}$ vs. q^2, where $\bar{\Gamma}$ is the average decay rate and q is the scattering vector, given by $q = (4\pi/\lambda) \sin(\theta/2)$, where λ is the incident wavelength and θ the scattering angle. Sample times were chosen so that the data extend to $\bar{\Gamma}t \approx 2$–4 and the correlation function had decayed to the base line. The multisample time capability was used to describe the early portion of the correlation function with the majority of the real-time channels. The advantage of this option stems from the effects of polydispersity on the correlation function, as discussed below.

Analysis of Correlation Functions. Recently, it was demonstrated that the shape of the autocorrelation function is strongly affected by the molecular weight distribution of the probe and the concentration of the matrix polymer.[29] Deviations from a single-exponential decay occur whenever there is a distribution of scattering particle mobilities. Even for relatively monodisperse samples, i.e., $M_w/M_n < 1.1$, these deviations can become severe in semidilute or concentrated solutions if the molecular weight dependence of Γ increases from $M^{-(0.5-0.6)}$ at infinite dilution toward the M^{-2} behavior characteristic of reptation. With recognition that this is a potential source of error, various methods to extract mean decay rates have been examined and the errors associated with each technique have been estimated from simulations. The techniques ultimately employed were two-term cumulants analysis, but emphasizing the early portion of the decay, and the Provencher inversion algorithm.[30]

In the homodyne case, the general expression relating the normalized scattered intensity and electric field autocorrelation functions, $C(t)$ and $g(t)$, respectively, is

$$C(t) = 1 + \gamma g^2(t) \tag{1}$$

where γ is typically in the range 0.1–0.3 for the solutions examined here. For a polydisperse system, $g(t)$ is the weighted sum of decay rates corresponding to the distribution of molecular weights in the scattering sample

$$g(t) = \int_0^\infty G(\Gamma) e^{-\Gamma t}\, d\Gamma \tag{2}$$

where the distribution of decay rates $G(\Gamma)$ may be expressed as

$$G(\Gamma) = \frac{\int_0^\infty Mw(M)\delta(\Gamma - \Gamma(M))\, dM}{\int_0^\infty Mw(M)\, dM} \tag{3}$$

where $w(M)$ is the weight fraction of scattering polymer with molecular weight M, and $\delta(x)$ is the Dirac δ function. In eq 3, it is assumed that $qR_g < 1$; i.e., the single-chain scattering factor is unity.

The actual molecular weight distribution may be approximated by the Schultz or log-normal distributions, and if the assumption is made that the decay rate can be written as $\Gamma(M) \sim M^\beta$, a series of dimensionless curves for $g(t)$ can be generated, given values for the power law exponent β and the polydispersity M_w/M_n. The computer-simulated autocorrelation functions may then be used to assess the accuracy and reliability of various fitting procedures by comparing the extracted average decay rate, Γ_{app}, to the known $\bar{\Gamma}$

$$\bar{\Gamma} = \int_0^\infty \Gamma G(\Gamma)\, d\Gamma \tag{4}$$

As an illustration, curves were generated for a polydispersity of 1.1, a preexponential factor γ of 0.25, and β values of −0.75, −0.98, and −1.91, which correspond to values observed in the experimental data. The simulated data were then analyzed, with the results summarized in Table I. For a given value of β, ratios of Γ_{app} to the true $\bar{\Gamma}$ are reported for one- (single-exponential), two-, and three-term cumulant expansion fits and the Provencher algorithm. Furthermore, the cumulant fits were repeated over different ranges of $2\bar{\Gamma}t$. In general, the cumulant approach is quite accurate: a two-cumulant fit gives a maximum 10% error and the accuracy is improved significantly by increasing the number of terms in the series expansion or by fitting only the earliest portion of the decay curve. However, the normalized second cumulant, or quality factor ($\mu_2/\bar{\Gamma}^2$), cannot be used as a simple

Table I

	β = −0.75			β = −0.98			β = −1.91		
$2(\Gamma t)_{max}$	5	3	1.5	5	3	1.5	5	3	1.5
				$\Gamma_{app}/\Gamma_{true}$					
CONTIN	0.999			0.996			1.000		
1-CUM	0.973	0.973	0.976	0.954	0.954	0.959	0.824	0.826	0.848
2-CUM	0.997	0.998	0.999	0.994	0.994	0.997	0.923	0.936	0.960
3-CUM	1.000	1.000	1.000	0.999	0.999	1.000	0.966	0.975	0.987
				$\gamma_{app}/\gamma_{true}$					
CONTIN	1.000			0.999			1.000		
1-CUM	0.992	0.992	0.994	0.987	0.987	0.990	0.950	0.950	0.962
2-CUM	1.000	1.000	1.000	0.999	0.999	1.000	0.983	0.988	0.994
3-CUM	1.000	1.000	1.000	1.000	1.000	1.000	0.994	0.996	0.999
				μ_2/Γ^2_{true}					
2-CUM	0.045	0.045	0.047	0.073	0.073	0.078	0.176	0.195	0.238
3-CUM	0.052	0.052	0.052	0.088	0.090	0.096	0.278	0.303	0.350
TRUE		(0.054)			(0.096)			(0.466)	

Table II
Diffusion Coefficients for PS in PVME, $P = 1.3 \times 10^6$

$M = 6.5 \times 10^4$		$M = 1.79 \times 10^5$		$M = 4.22 \times 10^5$		$M = 1.05 \times 10^6$	
log c	log D	log c	log D	log c	log D	log c	log D
−3.001	−6.26	−3.000	−6.53	−2.997	−6.72	−3.009	−6.91
−2.857	−6.25	−2.854	−6.55	−2.853	−6.75	−2.858	−6.94
−2.688	−6.26	−2.700	−6.57	−2.694	−6.79	−2.705	−6.98
−2.523	−6.32	−2.527	−6.62	−2.524	−6.83	−2.526	−7.06
−2.398	−6.35	−2.395	−6.64	−2.393	−6.89	−2.399	−7.11
−2.221	−6.38	−2.223	−6.69	−2.225	−6.97	−2.222	−7.20
−2.097	−6.42	−2.098	−6.75	−2.097	−7.05	−2.101	−7.30
−2.000	−6.46	−2.004	−6.84	−2.003	−7.11	−2.012	−7.39
−1.857	−6.54	−1.852	−6.95	−1.861	−7.24	−1.862	−7.57
−1.699	−6.64	−1.697	−7.11	−1.699	−7.45	−1.706	−7.80
−1.532	−6.73	−1.521	−7.29	−1.523	−7.75	−1.530	−8.17
−1.398	−6.88	−1.396	−7.44	−1.398	−7.94	−1.403	−8.47
−1.214	−7.05	−1.219	−7.80	−1.215	−8.36	−1.219	−8.98
−1.097	−7.21	−1.105	−8.10	−1.100	−8.75	−1.100	−9.37
−1.000	−7.33	−1.000	−8.29	−1.003	−8.83	−1.009	−9.65
				−0.959	−9.11	−0.951	−9.81

measure of polydispersity in the semidilute region. Although small, as expected, at $\beta = -0.75$, the quality factor is sensitive to the molecular weight exponent and the fitting parameters and can become large (e.g., $\gtrsim 0.2$) when β approaches −2. In addition, the larger values of $(\mu_2/\bar{\Gamma}^2)$ are not in good agreement with the true values. Values of Γ_{app} obtained via the Provencher algorithm are also in excellent agreement with $\bar{\Gamma}$, and the distribution of decay rates increases with β, as expected. Simulations with other values of γ indicated that Γ_{app} is essentially independent of γ. These simulations were repeated with the addition of various amounts of random noise; the results in Table I were all independent of the root-mean-square noise amplitude.

These simulations were performed with exact knowledge of the base-line value. Thus, caution is necessary in applying these techniques to real data. For example, increasing the number of terms in the cumulant expansion or severely limiting the range of $\bar{\Gamma}t$ sampled will not necessarily improve the results. To extract Γ_{app} from experimental data, three base-line options may be considered: the theoretical, or calculated base line, computed directly from the average scattered intensity; the measured, or experimental base line, which for this correlator is the average value of four delay channels (delayed by 1029 times the initial sample time); a "floating" base line, left as a free parameter in the fit. In general, the calculated base line is the correct one and should be used whenever possible. Furthermore, comparison of measured and calculated base lines is frequently an excellent test for dust contamination. The results from cumulant analysis in Table I were obtained with the base line fixed to the correct value. However, if the base line is allowed to "float", the regression tends to stabilize to a slightly higher base-line value. As a result, the "base-line-floated" Γ_{app} is closer to the true value than when the base line is fixed. This observation can be understood in terms of the extremely long tails in the simulated correlation functions, resulting from the breadth of $G(\Gamma)$. In essence, the floating base line serves as an extra parameter to compensate for the finite number of cumulant terms in the fitting function. Thus, for relatively large molecular weight exponents (i.e., $\beta < -1$), where the terms in the cumulant series do not converge rapidly, floating the base line may actually be justified.

The experimental data were consistently fit to a two-cumulant expression, comparing the values for the theoretical, measured, and floated base line. Typical values of 0.1–0.6% were obtained for the difference between the calculated and measured base lines, and data with greater than a 1% difference were discarded. Sample times were selected so that the decay curve extended to $\bar{\Gamma}t \sim 2.5$, and the sampling window was scaled to each angle in a given set of data. The necessity of this procedure results from the trends observed in Table I; maintaining a constant $\bar{\Gamma}t = 2.5$ minimizes errors associated with changes in the range of scaled time $\bar{\Gamma}t$ that is sampled. Furthermore, the multiple sample time option was used to concentrate the data in the early portion of the decay, as suggested by the results in Table I. The reported D values were obtained from the slope of (linear) plots of $\bar{\Gamma}$ (measured base line) vs. q^2. As a cross check, values of $\bar{\Gamma}$ from the Provencher algorithm were compared for randomly selected decay curves; the values were always within 10% of the cumulant values. Thus, the uncertainty in all reported D values is estimated to be 10% or less. In general, the Provencher results indicated a unimodal $G(\Gamma)$, although occasionally a small amount of a faster decay mode appeared. Because its amplitude was small, inclusion or rejection of this faster component did not have an appreciable effect on $\bar{\Gamma}$. However, as suggested previously,[29] the experimental concentration dependence of the breadth of $G(\Gamma)$ is not in perfect agreement with the predictions of the polydispersity analysis. Hence, it is possible that there is some multimodal character to $G(\Gamma)$ in these solutions, but if so, it is not clearly resolved.

Results

The measured diffusion coefficients for the four PS molecular weights are plotted vs. PVME concentration in

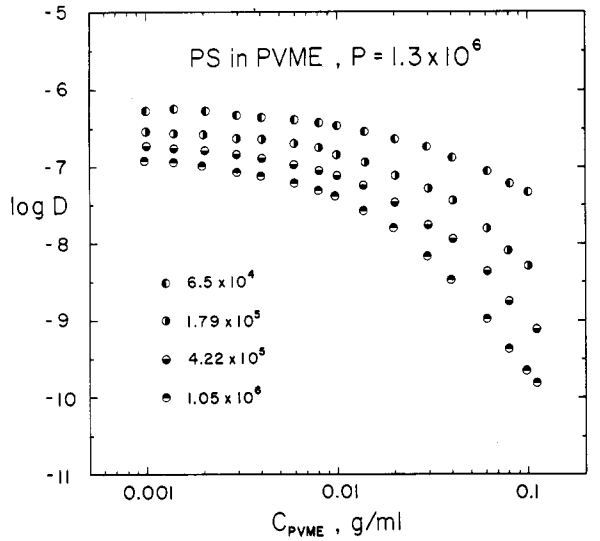

Figure 1. Diffusion of tracer PS chains in PVME/o-FT solutions.

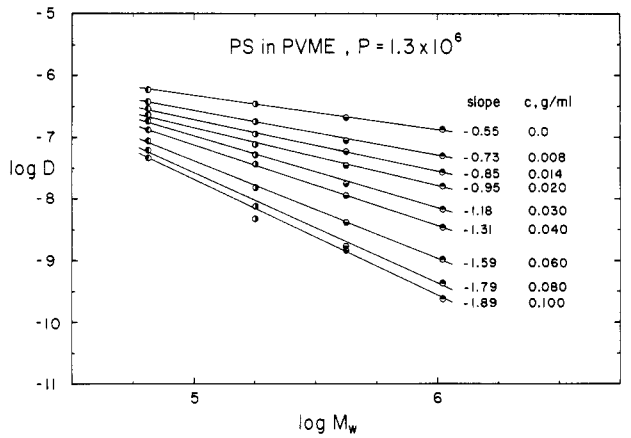

Figure 2. PS molecular weight dependence of diffusion.

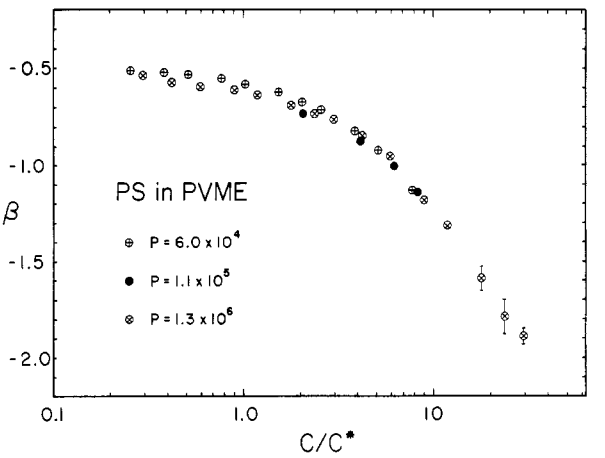

Figure 3. PS molecular weight exponent for diffusion as a function of reduced PVME concentration.

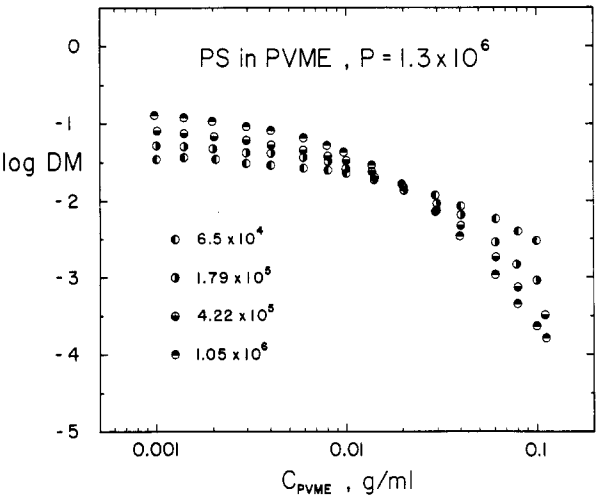

Figure 4. PS diffusion scaled as DM vs. PVME concentration.

Figure 1 and are listed in Table II. The D values extend over 4 orders of magnitude and decrease smoothly while the concentration varies over 2 decades. The PS molecular weight and PVME concentration dependencies of the data are more clearly revealed by plotting in several alternate formats. In Figure 2, D is plotted as a function of M_{PS} (henceforth, $M = M_{PS}$), at fixed values of c_{PVME}. It can be seen that within the uncertainty in the data, D follows a power-law dependence on M with the exponent β a decreasing function of c_{PVME}. In Figure 3, these exponents are plotted as a function of reduced concentration c_{PVME}/c^*_{PVME}, where c^* is taken to be 0.003 34 g/mL (= $1.5/[\eta]$) for this matrix. Also included in this plot are exponents obtained in a similar fashion from PS diffusion in other PVME matrices with lower molecular weights.[22,23] The relevant values of c^* were obtained by scaling from 0.00334 g/mL by the factor $(P)^{-0.8}$ ($P = M_{PVME}$), as o-FT is a good solvent for PVME. Note that the data of Martin (where $P = 1.1 \times 10^5$) were obtained in toluene.[23] Because toluene is also a good solvent for PVME and has a viscosity very close to that of o-FT, these data should be directly comparable. Within the precision of the data, reduction to a master curve is observed, with the exponent decreasing to −1.9 at a reduced concentration of 30. This suggests that reptation is not the dominant mechanism for diffusion in these systems, at least until concentrations well beyond coil overlap. However, −1.9 is close to −2, and thus these data may reflect the onset of a reptation regime.

An alternative means of examining the molecular weight dependence of diffusion is to plot log (DM^b) vs. log c_{PVME}, where b is a selected exponent. In a concentration regime where b is chosen "correctly", reduction to a master curve will be observed; however, the log–log format has a tendency to mask the details revealed by the approach of Figures 2 and 3. In a previous report describing the $P = 6 \times 10^4$ data, a plot of log DM vs. log c_{PVME} implied the existence of a "Rouse" regime (i.e., $D \sim M^{-1}$) at intermediate concentrations.[21] Similar general observations of the screening of hydrodynamic interaction with increasing concentration are well-known in conformational dynamics experiments.[31,32] However, when the data presented here are plotted according to this format, as in Figure 4, the coincidence of the curves occurs only at a point, rather than over a range of concentration. Because the Rouse model attempts to describe the dynamics of a single, isolated chain, Figure 4 should be taken as emphasizing that any description of finite concentration solution behavior as "Rouse-like" is at best only qualitative.

The concentration dependence of the diffusion data are examined by considering reduced plots of log (D/D_0) against log c_{PVME}/c^*_{PS}, where D_0 is the infinite dilution diffusion coefficient for PS in o-FT. It is important to note that in this instance the concentration axis is reduced by the overlap concentration of the PS component, to account for the differences among the PS hydrodynamic radii relative to the matrix "mesh size", at a given c_{PVME}. Because o-FT is a good solvent for PS, one might anticipate that c^*_{PS} should be calculated accordingly. The results of such a reduction are shown in Figure 5; a master curve is clearly not obtained. However, Figure 6 reveals that if the

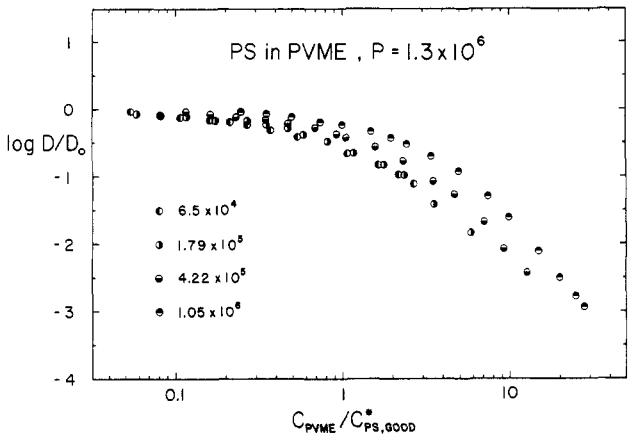

Figure 5. Reduced PS diffusion vs. PVME concentration scaled by c^* for PS, estimated by assuming good solvent conditions.

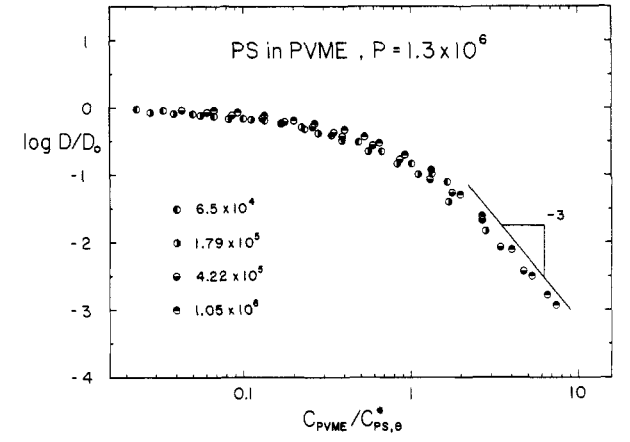

Figure 6. Reduced PS diffusion vs. PVME concentration scaled by c^* for PS, estimated by assuming Θ solvent conditions.

PVME/*o*-FT solution is taken as an effective Θ solvent, and thus $c^*_{PS} \sim M^{-0.5}$, a reasonable master curve is obtained. One implication of this observation is that the PS coil dimensions in *o*-FT begin to contract as soon as PVME is added, so that before the coil overlap concentration is attained, the individual PS coils have achieved near-Θ dimensions. This is in contrast to binary PS/good solvent solutions, where the contraction toward the bulk, unperturbed dimensions is expected to occur largely at concentrations greater than c^*.[2,33] In the high concentration region of Figure 6, a straight line of slope −3 has been drawn for comparison with the data, in accordance with the predictions of scaling theory coupled with reptation, for a Θ solvent. The agreement is quite good, but it must be borne in mind that the range of concentration involved is not great. As with the molecular weight dependence, this observation may reflect the onset of a reptation regime.

Prior to discussion of these results in more detail, it is important to consider possible differences between the measured diffusion coefficient, D, and the true translational diffusion coefficient of an isolated PS chain in the PVME matrix, D_{PS}. By analogy with dynamic light scattering in dilute binary solutions, the appropriate relationship is

$$D = D_{PS}[1 + k_D c_{PS} + ...] \quad (5)$$

where k_D accounts for the effects of the small but finite PS concentrations necessary to perform the measurements. The quantity D_{PS} may be further separated into the product of D_0 and an unknown function of M, P, and c_{PVME}; gaining insight into this unknown function is the main goal of the study. Potential subtle difficulties arise from two sources: first, k_D is an unknown function of c_{PVME}, M, and quite possibly P, and, second, the PS coil radius can also depend on c_{PVME}. The latter possibility could be viewed as effectively making D_0, used as a normalization constant in Figures 5 and 6, a function of c_{PVME}. Direct quantitation of both effects by scattering measurements is possible but very laborious. Preliminary measurements of k_D reveal that for the 1.05×10^6 PS sample, k_D decreases from 80 mL/g in pure *o*-FT to −20 mL/g in a 0.04 g/mL solution of PVME ($P = 6.3 \times 10^5$). Corresponding values of 160 and −60 are obtained by interpolation of published results for PS in THF[34] and cyclohexane.[35] This indicates that the effect can be significant and, more importantly, supports the inference, drawn from Figure 6, that the ternary solutions are effectively Θ solvents for the PS.

Discussion

The molecular weight dependence of translational diffusion displayed in Figures 2 and 3 suggests that reptation is not the primary contributor to the net diffusion rate, up to reduced matrix concentrations c_{PVME}/c^*_{PVME} of at least 10. The observation of molecular weight exponents between −1 and −2 in the semidilute regime has also been reported by other workers.[5,7,22,23,36] Computer simulation of translational diffusion over the complete concentration range also revealed a smooth variation of exponent, with a minimum value of −1.7; (no hydrodynamic interaction was included in this model, so the dilute solution limiting value was −1).[37] Of particular interest in the results reported here is the observation that the diffusion coefficient follows a molecular weight power law at all concentrations studied. This suggests that at any given matrix concentration a single diffusion mechanism (or combination of mechanisms) is (are) operative, for all diffusant molecular weights. Thus, this mechanism, or combination of mechanisms, in these solutions is independent of whether the ratio of the diffusant dimension, R, to the mesh size, ξ, is greater or less than unity. This is in conflict with the simple picture of a semidilute solution as being characterized by a single dynamic length scale. For example, at some intermediate concentration, the lower M PS molecules have $R < \xi$, while the higher M molecules have $R > \xi$; in the simplest scaling picture, these two regimes should be characterized by different molecular weight exponents, which is not indicated by the data. This observation may reflect the existence of multiple characteristic length scales in semidilute solutions, leading to behavioral regimes that are not clearly resolved. The existence of multiple dynamic length scales has also been deduced on the basis of extensive dynamic light scattering measurements on binary semidilute solutions; multimodal correlation functions have been observed over wide ranges of concentration (above c^*) for good, Θ, and marginal quality PS solutions.[38-40] However, as discussed previously, in the data reported here there was no direct evidence of multimodal character in the correlation functions. As an alternative explanation, the ratio of R for the largest PS to that of the smallest considered here is approximately 4 and thus may not differ sufficiently to define the regimes $R > \xi$ and $R < \xi$ clearly.

It should be emphasized that the polydispersity of the matrix may be a crucial factor in these results, serving to smooth out any distinctive features in the diffusion process by providing an essentially continuous distribution of matrix relaxation times. Thus, while the gross features of the molecular weight and concentration dependence of diffusion are revealing, it is probably not appropriate to infer much about the structure of semidilute solutions of

monodisperse polymers. Polydispersity effects may also account for the difference between these results and the extensive forced Rayleigh scattering measurements of semidilute PS/toluene solutions recently reported by Yu et al.[7] In their diffusion data, power-law behavior did not extend over a wide range of diffusant molecular weight, and apparent molecular weight exponents (i.e., tangents) down to −3 were reported. An additional distinction between the two studies involves the effect of matrix molecular weight, as will be discussed subsequently.

The concentration range examined here extends up to approximately 10% polymer, which may be taken as a rough demarcation between semidilute and concentrated regimes. One advantage of operating over this range is that, since the solvent volume fraction is so high, the concentration dependence of the monomeric friction coefficient can be neglected, as has been demonstrated for several systems.[29,41,42] The crucial disadvantage in this instance is the fact that the continuing evolution of the molecular weight exponent is not observed; the method of solution preparation (i.e., most concentrated first) effectively prohibits extension of the measured concentration range with these solutions. Over the measured concentration range, a molecular weight exponent of −2 is not observed. The Stokes–Einstein mechanism, operative in dilute solution, is superseded at c^* for the matrix, as indicated by the loss of superposition in a plot of D/D_0 vs. c (not shown). Thus, even if reptation is assumed at concentrations beyond the measured range, there is a substantial interval of matrix concentration for which no simple picture of diffusion may suffice, and other mechanisms need to be invoked. In fact, within the indicated uncertainty in the exponent values in Figure 3, there is not evidence of a leveling off at the reptation limit of −2. This is interesting in light of the recent formulation of entangled solution dynamics in terms of the so-called "noodle effect", in which single chains drag portions of constraining chains for finite distances; this leads to a predicted molecular weight exponent of −2.5.[10] Thus, although these semidilute data are not explainable in this manner either, it might be argued that the exponent appears to be heading beyond −2. On the other hand, the noodle effect also predicts a concentration exponent of −1.5, which is clearly an underestimate at the higher concentrations.

It has been established that coil overlap does not guarantee intermolecular entanglement, in the viscoelastic sense, and thus it is instructive to examine these data in terms of the concentration for the onset of entanglement, c_e.[31] This may be estimated as $\rho M_c^0/M$, where ρ is the polymer density and M_c^0 is the critical molecular weight for the onset of the $M^{3.4}$ dependence of the melt shear viscosity. In this manner, c_e for the matrix is estimated as 0.011 g/mL, using a value of 14 400 for P_c^0;[43] thus, approximately 50% of the reported data fall in the entangled matrix regime. However, it is equally important to consider the corresponding c_e values for the diffusant polymers. When M_c^0 is taken to be 35 000, values of 0.57, 0.21, 0.087, and 0.035 g/mL are obtained for the four PS samples, in order of increasing M. Thus, only the largest of the four is entangled with the matrix over a significant fraction of the measured concentration range. If intermolecular entanglement estimated in this manner is a necessary precursor to the onset of a reptation regime, then the absence of a molecular weight exponent of −2 in the measured range is completely understandable. (Just as with c^*, there is some arbitrariness in the numerical estimation of c_e; for example, M_e^0 might be used in place of M_c^0, reducing c_e values by approximately a factor of 2.[31,41] This would have no effect on the conclusions presented here, however.)

A ternary solution with chemically dissimilar polymers is not a simple thermodynamic system. However, in our interpretation of the probe diffusion data, any thermodynamic complexity has been tacitly ignored. This is justifiable on several grounds: (i) in the limit $c_{PS} \to 0$, the driving force for PS diffusion is entropic, and no macroscopic chemical potential gradients exist; (ii) the distance scales probed are consistently larger than molecular dimensions, and thus the details of any styrene–vinyl methyl ether monomer–monomer interactions that may influence the dynamics are averaged out; (iii) the observed compatibility of the ternary system over a wide range of M, P, and composition suggests that the measurements are not being made in close proximity to any phase boundaries; (iv) the absolute magnitudes of the measured diffusion coefficients have been shown to be very similar to those obtained in binary solutions by other techniques.[3,20,22] However, some interesting thermodynamic questions remain. For example, do the PS coil dimensions vary with c_{PVME}? The results reported here suggest, albeit indirectly, that a contraction occurs with increasing c_{PVME}. On the other hand, Martin has argued that the chemical difference between PS and PVME chains will preserve intramolecular excluded volume interactions over all length scales for the trace PS chains.[44] In his calculation, rederived as a special case below, a reptation exponent of −1.8 is predicted; this is clearly not supported by these data.

The original postulate of reptation concerned the motion of linear chains through a fixed matrix, such as a crosslinked network. For diffusion in melts and solutions, therefore, it is necessary to account for the mobility of the matrix chains; one route to this is via the mechanism of "tube renewal" or "constraint release".[8,9,45,46] Various calculations based on constraint release may differ in certain details, but the essence of the process is that a test chain is able to translate laterally when a constraining chain diffuses away, presumably by reptation. A straightforward experimental test for the occurrence of constraint release is to measure the diffusion coefficient of a test chain while increasing the matrix molecular weight. Pure reptation requires independence of matrix size (P), whereas constraint release has a strong ($\sim P^{-3}$) dependence. In melts, there is evidence for the necessity of accounting for the constraint release contribution;[8,9] in solution, the situation is not at all clear. While the addition of solvent molecules to a melt certainly enhances the mobility of matrix chains, the constraint release mechanism referred to above in effect presupposes that reptation is the primary transport mechanism, which is in conflict with the data in this study. Yu et al. have shown that in semidilute solutions the diffusion coefficient of a test chain (M) does not become independent of matrix molecular weight until $P \approx 3$–$5M$; furthermore, the factor of 3–5 does not depend on matrix concentration.[7] On this basis, recognizing that a PVME matrix with $P = 1.3 \times 10^6$ corresponds in degree of polymerization to a PS of $M \approx 2.2 \times 10^6$, the larger two PS diffusion coefficients may not have reached their infinite matrix molecular weight values D_∞, and thus the observed molecular weight exponents may reflect a weaker M dependence than D_∞. On the surface, this might appear to be evidence for constraint release, but the scaling argument outlined below indicates that these data cannot be interpreted as a combination of reptation and constraint release in a self-consistent manner. A similar conclusion was reached by Yu et al. from their data.[7]

Table III
Ternary Solution Reptation Exponents $D \sim M^i P^j c^k$

x	μ	ν	i	j	k
1.0	0.5	0.5	−2	0	−3
1.0	0.6	0.5	−2	0	−2.33
1.0	0.5	0.6	−2	0	−2.25
1.0	0.6	0.6	−2	0	−1.75
1.2	0.5	0.5	−1.8	0	−2.6
1.2	0.6	0.5	−1.8	0	−2.0
1.2	0.5	0.6	−1.8	0	−1.95
1.2	0.6	0.6	−1.8	0	−1.5

The following calculations are simple extensions of previous developments for calculating the molecular weight and concentration dependence of diffusion by reptation and constraint release, here applied to the case of a single test chain of length M in a matrix of P chains. It is assumed that both M and P are larger than their respective entanglement lengths, and that the concentration of P is such that the P solution is semidilute and the M chain is larger than the mesh size ξ. The starting point is the concentration dependence of the mesh size, given by[2]

$$\xi \sim c^{\nu/(1-3\nu)} \tag{6}$$

where ν reflects the solvent quality for the P chains and is 0.5 in a Θ solvent and 0.6 in a good solvent. The mesh size may be taken to define a "blob", or the length scale over which the solvent power is still important. Over distances larger than ξ, any chain is taken to have the dimensions of a Gaussian chain of blobs. The number of monomers in a blob is given by

$$P_b \sim c(\xi)^3 \sim c^{1/(1-3\nu)} \tag{7a}$$

$$M_b \sim c(\xi)^3 \sim c^{\nu/\mu(1-3\nu)} \tag{7b}$$

where the exponent μ recognizes that the solvent quality may be different for the M chain. The reptation diffusion coefficient for an M chain, D_{rep}, is calculated as $R_g^2(M)/T_{rep}$, with T_{rep} the reptation time for an M chain. T_{rep} is taken as L^2/D_t, where L is the tube length and D_t is the longitudinal diffusion coefficient along the tube. The radius of gyration of the M chain may be written as

$$R_g^2 \sim (M/M_b)^x(\xi)^2 \tag{8}$$

where the exponent x allows for the possibility that a chemical difference between M and P chains will preserve the excluded volume statistics of the M chain over distances larger than ξ. In this case $x = 1.2$, while in the traditional picture $x = 1$. The results are

$$T_{rep} \sim P^0 M^3 c^{-3\nu/\mu(1-3\nu)} c^{3\nu/(1-3\nu)} \tag{9}$$

and

$$D_{rep} \sim P^0 M^{x-3} c^{(3-x)\nu/\mu(1-3\nu)} c^{-\nu/(1-3\nu)} \tag{10}$$

The resulting exponents are listed in Table III for the limiting cases of good and Θ solvents for each component. Note that if $\mu = \nu$ and $x = 1$ the well-known results for binary semidilute solutions are recovered and that taking $x = 1.2$ leads to the $M^{-1.8}$ prediction referred to earlier.

The calculation of the constraint release diffusion coefficient, D_{cr}, proceeds in the same spirit following the arguments of Klein.[47] D_{cr} is taken as R_g^2/T_{cr}, where the constraint release time is given as

$$T_{cr} \sim T_1(M,c) T_{rep}(P,c) \tag{11}$$

with T_1 the longest relaxation time of the tube and T_{rep} the time for a P chain to reptate away. The tube relaxation time is calculated by analogy with dilute solution:

$$T_1 \sim (M/M_b)^y \tag{12}$$

where $y = 1.5$ for a hydrodynamically unscreened ("Zimm") tube and $y = 2$ for a screened ("Rouse") tube. It has been argued that the former case is more reasonable,[47] but both possibilities have been retained for completeness. The resulting expression for the diffusion coefficient is

$$D_{cr} \sim P^{-3} M^{x-y} c^{(y-x)\nu/\mu(1-3\nu)} c^{(3-\nu)/(1-3\nu)} \tag{13}$$

Table IV
Ternary Solution Constraint Release Exponents $D \sim M^i P^j c^k$

x	μ	ν	y	i	j	k
1.0	0.5	0.5	1.5	−0.5	−3	−6.0
			2.0	−1.0	−3	−7.0
1.0	0.6	0.5	1.5	−0.5	−3	−5.83
			2.0	−1.0	−3	−6.66
1.0	0.5	0.6	1.5	−0.5	−3	−3.75
			2.0	−1.0	−3	−4.5
1.0	0.6	0.6	1.5	−0.5	−3	−3.625
			2.0	−1.0	−3	−4.25
1.2	0.5	0.5	1.5	−0.3	−3	−5.6
			2.0	−0.8	−3	−6.6
1.2	0.6	0.5	1.5	−0.3	−3	−5.5
			2.0	−0.8	−3	−6.33
1.2	0.5	0.6	1.5	−0.3	−3	−3.45
			2.0	−0.8	−3	−4.2
1.2	0.6	0.6	1.5	−0.3	−3	−3.375
			2.0	−0.8	−3	−4.0

and the resulting exponents are listed in Table IV. As with the reptation results, the subtleties of the solvent quality and the tube dynamics do not affect the P dependence, while the M dependence varies somewhat. In all cases, the M dependence is weaker than for reptation, which suggests that an appropriate combination of D_{rep} and D_{cr} could match the M dependence observed in the semidilute regime. However, for the concentration dependence this is not possible. In all cases, the concentration dependence of D_{cr} is stronger than for D_{rep}, whereas the observed dependence is generally weaker. Furthermore, as concentration decreases, the M dependence implies a larger weighting of D_{cr} while the c dependence implies the opposite. The basis for the stronger c dependence of D_{cr} is clear: the reptation c dependence for a reptating P chain is coupled to the c dependence of the number of blobs in the tube. The physical reason for the failure of this mechanism to mimic the features of diffusion in the semidilute regime was alluded to above, namely, the constraint release assumes a P chain moves primarily *by reptation*; thus, when the M and P chains are linear and of comparable length, constraint release can never be substantial contribution relative to reptation without violating its own definition. This argument should not be interpreted as saying that matrix mobility is not important in solution; on the contrary, how to describe the matrix mobility may in fact be the key issue. The preceding calculations are presented primarily to illustrate the point that diffusion in semidilute solutions cannot be described by a linear combination of reptation and constraint release, in a self-consistent manner. Given the apparent failure of the corresponding developments for binary semidilute solutions to describe or reconcile all the experimental data, it is certainly not expected that the various predictions in Tables III and IV will agree with experimental observations.

It has recently been suggested that an empirical equation is quite successful in describing the concentration depen-

Table V
Parameter Values from Eq 15

	measured values			floated values		
M	D_0	a^a	u	D_0	a	u
6.5×10^4	5.98×10^{-7}	0.125	0.66	7.10×10^{-7}	0.201	0.57
1.79×10^5	3.51×10^{-7}	0.167	0.72	3.59×10^{-7}	0.176	0.71
4.22×10^5	2.11×10^{-7}	0.226	0.69	3.00×10^{-7}	0.375	0.59
1.05×10^6	1.36×10^{-7}	0.347	0.64	2.11×10^{-7}	0.437	0.60
$3.79 \times 10^{5\,b}$	2.24×10^{-7}	0.191	0.71	3.02×10^{-7}	0.304	0.62
$1.19 \times 10^{6\,b}$	1.19×10^{-7}	0.300	0.72	1.91×10^{-7}	0.471	0.63

[a] Concentrations entered as mg/mL. [b] 3-arm star.

dence of diffusion in the semidilute regime.[18] The expression may be written as

$$D/D_0 = \exp\{-\alpha c^u R^v P^w\} \quad (14)$$

where c, R, and P refer to the matrix concentration, probe radius, and matrix molecular weight, respectively. To emphasize the concentration dependence, eq 14 may be simplified to

$$D/D_0 = \exp\{-ac^u\} \quad (15)$$

This functional form has been compared to diffusion data on a variety of systems, with the probes including globular proteins,[17] latex spheres,[17] colloidal particles,[11,16] flexible linear polymers,[18] and 12-arm star polystyrenes,[27] in dilute and semidilute polymer solutions. In general, the data from these quite disparate systems are all describable via eq 15, with values of u ranging from 0.5 to 1. Though as yet lacking a firm basis in statistical mechanics, the exponential form has a certain amount of theoretical justification, arising from the increase of many-particle hydrodynamic interactions with increasing concentration. Different treatments lead to predictions for the concentration exponent u of 0.5,[11,14] 0.75,[13] and 1;[12] each approach may thus derive some support from the data reported hitherto. The apparent universality of the equation admits of at least two explanations. It may reflect either that the essential physics of the diffusion process is the same in all cases or that the so-called stretched exponential form is sufficiently pliable to describe the range of reported data. If the former is the case, the primary implication is that the characteristics of the matrix are the main determinant of the diffusion mechanism and that, in particular, reptation is not important for linear polymers in semidilute solutions.[18] In the latter case, the equation may serve as a useful means to describe and compare diffusion data, but at the same time any information concerning the underlying physics may be obscured.

In order to assess these possibilities, the data of Figure 1 have been fit to eq 15, with a and u as adjustable parameters. The value of D_0 may be taken as that obtained via extrapolation of dilute, binary PS/o-FT solution data or it may also be left as an adjustable parameter; both approaches have been tried. Use of the measured value of D_0 should provide a more stringent test of the functional form, but the possible concentration dependence of D_0 discussed previously may to some extent legitimize the second approach. In Figure 7 are shown the results of the fit with an adjustable D_0. In general, the curves agrees remarkably well with the data, given an estimated uncertainty of 10% for each diffusion coefficient. However, closer inspection of the fit, particularly for the largest PS sample, reveals that the residuals of the fit are not randomly distributed about zero, suggesting that the data are not really conforming to this form. Figure 8 reveals that the agreement between the data and the fits with the experimental D_0 is noticeably worse, as might be expected given one less adjustable parameter. The resulting values

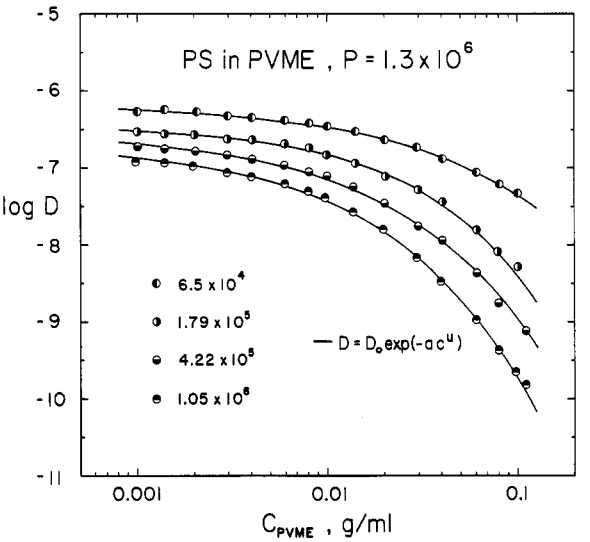

Figure 7. PS diffusion data fit to eq 15 with floating D_0.

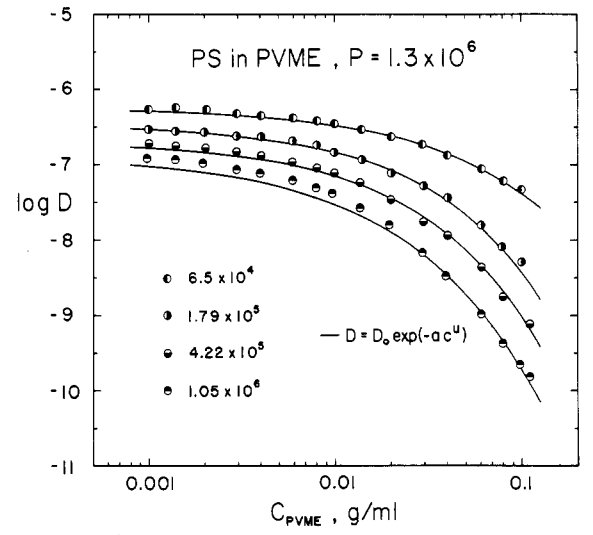

Figure 8. PS diffusion data fit to eq 15 with measured D_0.

of a, u, and D_0 are listed in Table V. The values of D_0 obtained by fitting are always larger than the measured ones, and the deviation generally increases with M. Both the magnitude and the direction of the changes are consistent with the postulated concentration dependence of D_0, but confirmation of this interpretation must await the completion of direct light scattering determination of the coil dimensions. The values of u are scattered in the range 0.57–0.71, which is in reasonable agreement with the concentration dependence of the hydrodynamic screening length obtained by dynamic light scattering on binary semidilute solutions.[48]

In general, it appears that the form of eq 15 is capable of describing the concentration dependence of the data, within the uncertainty engendered by the value of D_0.

However, an interesting feature of this fit is revealed by comparing the results obtained with the diffusion of two 3-arm star PS molecules in the same matrix polymer.[49] The molecular weights of the stars were 3.79×10^5 and 1.19×10^6, and thus the data were compared to the two larger PS molecules of this study. The main result was that the smaller star diffused more rapidly than the corresponding linear molecule, over the range $0.001 < c_{PVME} < 0.1$ g/mL, while the larger star diffused up to an order of magnitude more slowly than the 1.05×10^6 linear PS, by the highest matrix concentration. These results were interpreted as indicating that topology was very important in determining the diffusion rates when the diffusant was substantially entangled with the matrix but that overall hydrodynamic dimensions determine the diffusion rates for a considerable range of concentration above the coil overlap. However, if the 3-arm star data are fit to eq 15 with adjustable D_0, values of 0.304 and 0.471 for a, and 0.62 and 0.63 for u were obtained, for the smaller and the larger star, respectively, as shown in Table V. Examination of these numbers reveals that the star values are well within the range of the linear values, suggesting similar diffusion mechanisms are operative. In particular, for the larger star and the largest linear PS, the difference in u (0.63 vs. 0.60) and a (0.471 vs. 0.437) are small enough to appear insignificant relative to the entire range of values in Table V. This stands in contrast to the clear difference in diffusion behavior. We are thus led to conclude that the apparent success of eq 15 in describing these data reflects more the flexibility of the stretched exponential form than the universality of probe diffusion mechanisms in semidilute solutions.

Conclusions

Translational diffusion coefficients of trace amounts of linear polystyrenes with molecular weights ranging from 6.5×10^4 to 1.05×10^6 have been measured in poly(vinyl methyl ether)/*o*-fluorotoluene matrices by dynamic light scattering. The matrix molecular weight, 1.3×10^6, and concentration range, 0.001–0.1 g/mL, were such that the data spanned the dilute and semidilute regimes, as well as the unentangled/entangled transition. The polystyrene diffusion coefficients followed a molecular weight power law at all concentrations, with the exponent varying smoothly from −0.55 at infinite dilution to −1.9 at the highest matrix concentration, corresponding to a reduced matrix concentration c/c^* of 30. It is not clear from these data whether the exponent was tending toward an asymptote of −2, in accordance with the reptation model, or whether it would become even larger in magnitude. The observation of a single power law at all matrix concentrations argues against the characterization of semidilute solutions by a single length scale; however, the somewhat limited range of probe dimension and the matrix polydispersity may conspire to obscure some features of semidilute diffusion behavior. Attempts to collapse the data to a master curve failed when the overlap concentration was chosen as c^* for polystyrene, assuming good solvent conditions; however, when Θ conditions were assumed, a reasonable universal curve was obtained. This observation suggests that the polystyrene coils undergo contraction upon the addition of matrix polymer, even though the solvent is thermodynamically good for both polymers. This interpretation is supported also by the fact that the diffusional virial coefficient, k_D, for the polystyrene changed sign with increasing matrix concentration.

The majority of the data fall in a regime where neither dilute solution Stokes–Einstein behavior nor reptation dominate; other mechanisms must be invoked, presumably centering on the mobility of the surrounding chains. However, a "Rouse" regime of screened hydrodynamic interaction is not observed. Furthermore, the mechanism of constraint release, apparently effective in describing certain features of melt diffusion, cannot be combined with reptation to describe these data. Thus, a straightforward molecular description of translational diffusion in semidilute solutions may not be possible. An empirical, stretched exponential form is reasonably successful in describing the concentration dependence of the data, but comparison of fitting parameters with those obtained for the diffusion of 3-arm star polystyrenes in the same matrix suggests that this success is due more to the flexibility of the fitting form. Consideration of the concentration necessary for the onset of entanglement, c_e, which is larger than the coil overlap concentration, c^*, indicates that $c > c_e$ is a minimum requirement for reptation to be effective. This is also in agreement with the conclusions drawn from the 3-arm star results.

Acknowledgement is made to the donors of The Petroleum Research Fund, administered by the American Chemical Society, and to the National Science Foundation, Grant CPE 8352364, for partial support of this research.

Registry No. PS, 9003-53-6; PVME, 9003-09-2.

References and Notes

(1) de Gennes, P.-G. *J. Chem. Phys.* **1971**, *55*, 572.
(2) de Gennes, P.-G. *Scaling Concepts in Polymer Physics*; Cornell University Press: Ithaca, NY, 1979.
(3) Tirrell, M. *Rubber Chem. Technol., Rubber Rev.* **1984**, *57*, 523.
(4) Leger, L.; Hervet, H.; Rondelez, F. *Macromolecules* **1981**, *14*, 1732.
(5) Callaghan, P. T.; Pinder, D. N. *Macromolecules* **1984**, *17*, 431.
(6) Wesson, J. A.; Noh, I.; Kitano, T.; Yu, H. *Macromolecules* **1984**, *17*, 782.
(7) Kim, H.; Chang, T.; Yohanan, J. M.; Wang, L.; Yu, H. *Macromolecules* **1986**, *19*, 2737.
(8) Green, P. F.; Kramer, E. J. *Macromolecules* **1986**, *19*, 1108.
(9) Bartels, C. R.; Crist, B., Jr.; Fetters, L. J.; Graessley, W. W. *Macromolecules* **1986**, *19*, 785.
(10) Fujita, H.; Einaga, Y. *Polym. J. (Tokyo)* **1985**, *17*, 1131.
(11) Ogston, A. G.; Preston, B. N.; Wells, J. D. *Proc. R. Soc. London A* **1973**, *333*, 297.
(12) Freed, K. F.; Edwards, S. F. *J. Chem. Phys.* **1974**, *61*, 3626.
(13) de Gennes, P.-G. *Macromolecules* **1976**, *9*, 594.
(14) Cukier, R. I. *Macromolecules* **1984**, *17*, 252.
(15) Altenberger, A. R.; Tirrell, M.; Dahler, J. S. *J. Chem. Phys.* **1986**, *84*, 5122.
(16) Langevin, D.; Rondelez, F. *Polymer* **1978**, *14*, 875.
(17) Phillies, G. D. J. *J. Chem. Phys.* **1985**, *82*, 5242.
(18) Phillies, G. D. J. *Macromolecules* **1986**, *19*, 2367.
(19) Hadgraft, J.; Hyde, A. J.; Richards, R. W. *J. Chem. Soc., Faraday Trans 2* **1979**, *75*, 1495.
(20) Lodge, T. P. *Macromolecules* **1983**, *16*, 1393.
(21) Hanley, B.; Balloge, S.; Tirrell, M. *Chem. Eng. Commun.* **1983**, *24*, 93.
(22) Hanley, B.; Tirrell, M.; Lodge, T. P. *Polym. Bull. (Berlin)* **1985**, *14*, 137.
(23) Martin, J. E. *Macromolecules* **1986**, *19*, 922.
(24) Numasawa, N.; Hamada, T.; Nose, T. *J. Polym. Sci., Polym. Phys. Ed.* **1986**, *24*, 19.
(25) Bank, M.; Leffingwell, J.; Thies, C. *Macromolecules* **1971**, *4*, 43.
(26) Kwei, T. K.; Nishi, T.; Roberts, R. F. *Macromolecules* **1974**, *7*, 667.
(27) Lodge, T. P.; Markland, P. *Polymer*, in press.
(28) Bauer, B. J.; Hanley, B.; Muroga, Y., in preparation.
(29) Lodge, T. P.; Wheeler, L. M.; Hanley, B.; Tirrell, M. *Polym. Bull. (Berlin)* **1986**, *15*, 35.
(30) Provencher, S. W.; Hendrix, J.; De Maeyer, L.; Paulussen, N. *J. Chem. Phys.* **1978**, *69*, 4273.
(31) Ferry, J. D. *Viscoelastic Properties of Polymers*, 3rd ed.; Wiley-Interscience: New York, 1980.
(32) Lodge, T. P.; Schrag, J. L. *Macromolecules* **1982**, *15*, 1376.
(33) Daoud, M.; Cotton, J. P.; Farnoux, B.; Jannink, G.; Sarma, G.; Benoit, H.; Duplessix, R.; Picot, C.; de Gennes, P.-G. *Macromolecules* **1975**, *8*, 804.
(34) Mandema, W.; Zeldenrust, H. *Polymer* **1977**, *18*, 835.
(35) Han, C. C. *Polymer* **1979**, *20*, 259.

(36) Tanner, J. *Macromolecules* **1971**, *4*, 748.
(37) Crabb, C.; Kovac, J. *Macromolecules* **1985**, *18*, 1430.
(38) Brown. W. *Macromolecules* **1985**, *18*, 1713.
(39) Brown, W. *Macromolecules* **1986**, *19*, 387.
(40) Brown, W. *Macromolecules* **1986**, *19*, 1083.
(41) von Meerwall, E. D.; Amis, E. J.; Ferry, J. D. *Macromolecules* **1985**, *18*, 260.
(42) Nemoto, N.; Landry, M. R.; Noh, I.; Kitano, T., Wesson, J. A.; Yu, H. *Macromolecules* **1985**, *18*, 310.
(43) Hashimoto, T., personal communication.
(44) Martin, J. E. *Macromolecules* **1984**, *17*, 1279.
(45) Daoud, M.; de Gennes, P.-G. *J. Polym. Sci., Polym. Phys. Ed.* **1979**, *17*, 1971.
(46) Klein, J. *Polym. Prepr. (Am. Chem. Soc., Div. Polym. Chem.)* **1982**, *22*, 105.
(47) Klein, J. *Macromolecules* **1986**, *19*, 105.
(48) Adam, M.; Delsanti, M. *Macromolecules* **1977**, *10*, 1229.
(49) Lodge, T. P.; Wheeler, L. M. *Macromolecules* **1986**, *19*, 2983.

Effect of Morphology on the Transport of Gases in Block Copolymers

David J. Kinning,† Edwin L. Thomas,* and Julio M. Ottino

Departments of Polymer Science and Engineering and Chemical Engineering, University of Massachusetts, Amherst, Massachusetts 01003. *Received August 11, 1986*

ABSTRACT: Transport studies of CO_2 in several solvent-cast poly(styrene-*co*-butadiene) block copolymers of controlled morphology are presented. The morphology is documented by means of transmission electron microscopy and the transport is examined by means of sorption. The transport properties predicted by simple models involving ordered microstructures agree surprisingly well with the experimental results. Transport studies are a sensitive measure of the connectedness of the most conductive phase (polybutadiene). By change of the composition of the copolymer or the casting solvent, the microdomain morphology, i.e., the connectedness of the polybutadiene domains, can be systematically changed. The variation in effective diffusion as a function of domain morphology is well captured by the models.

Introduction

The interaction of transport and morphology in multiphase polymer systems arises under many practical conditions, for example, in devolatilization in polymer blends and in the design of membranes, photographic films, coatings, packaging materials, and protective clothing, to name but a few. Nevertheless, there have been few combined studies of transport and morphology in multiphase polymer blends, with only simple diffusion and morphological models being considered.

Recently, Sax and Ottino[1] have presented models for predicting the effective diffusion coefficient of small-molecule gases in two-phase polymer blends exhibiting small-scale order but large-scale disorder. As shown in Figure 1 (reprinted from this work), for the case of alternating lamellar domains the structure is considered to consist of small (relative to the size of the sample) grains, in which there is a high degree of order, oriented randomly with respect to each other so that macroscopically the structure is isotropic. The models predict that the effective diffusion coefficient is not only a function of the volume fractions of the phases but also highly dependent on the domain morphology. Especially important in determining the transport behavior is the connectivity of the more diffusive (conductive) phase. Therefore, transport measurements can provide guidance in cases where other experimental techniques do not indicate which of the two phases is continuous. The models can predict the effective diffusion coefficient, D_{eff}, as a function of composition of spherical, cylindrical, and lamellar domains. These are exactly the type of domain structures often encountered for ordered block copolymers. Therefore, these materials should serve as model experimental systems with which to test the predictions of Sax and Ottino's models. In addition, when different casting solvents are employed, the domain morphology of block copolymers (i.e., the connectivity of the phases) can be systematically altered, enabling the effect of morphology on transport to be independently investigated.

Review of the Models

With the assumption of Fickian diffusion, the transport behavior within the small-scale ordered grain is assumed to be given by

$$\mathbf{J} = -\mathbf{D}\cdot\nabla C \tag{1}$$

where $\mathbf{J}$ is the flux vector, $\mathbf{D}$ is the diffusion tensor, and C is concentration. As shown by Sax and Ottino,[1] if there is random orientation of the grains the effective diffusion coefficient is given simply by the average of the diffusion coefficients in the principal directions

$$D_{eff} = (1/3)(D_{11} + D_{22} + D_{33}) \tag{2}$$

For example, in the alternating lamellar grains of Figure 1, the diffusion coefficients along the principal directions are given by

$$D_{11} = D_B([(1 - \Phi_B)/Sx + \Phi_B][S(1 + \Phi_B(1 - S)/S)])^{-1} \tag{3}$$

$$D_{22} = D_{33} = D_B[(1 - \Phi_B)Sx + \Phi_B]/[S(1 + \Phi_B(1 - S)/S)] \tag{4}$$

where Φ_A and Φ_B are the volume fractions of phases A and B, $S = S_A/S_B$, and $x = D_A/D_B$. S_A and S_B are the penetrant solubilities, and D_A and D_B are the penetrant diffusion coefficients in components A and B. Equations 3 and 4 were obtained by combining the classical results for electrical conductivity in layered domains (i.e., series and parallel laws) with the fact that the driving force for diffusion is the gradient of chemical potential rather than the gradient of concentration.[2] Solutions for the effective dielectric permeability of a dilute suspension of spheres[3] and a cubic lattice of cylinders[4] have also been presented, from which expressions for the effective diffusion coeffi-

† Current address: 3M Co., St. Paul, MN 55106.

0024-9297/87/2220-1129$01.50/0